IEEE Access
Multidisciplinary | Rapid Review | Open Access Journal

Received June 27, 2020, accepted July 6, 2020, date of publication July 14, 2020, date of current version July 27, 2020.

Digital Object Identifier 10.1109/ACCESS.2020.3009109

A Novel Stator Turn Fault Detection Technique by Using Equivalent High Frequency Impedance

BO WANG[1,2], (Member, IEEE), JIAPENG HU[1], GUANGHUI WANG[3], (Member, IEEE), AND WEI HUA[1], (Senior Member, IEEE)

[1]School of Electrical Engineering, Southeast University, Nanjing 210096, China
[2]Jiangsu Provincial Key Laboratory of Smart Grid Technology and Equipment, Nanjing 210096, China
[3]Department of Information and Control Technology, China North Vehicle Research Institute, Beijing 100072, China

Corresponding author: Bo Wang (bowang.ee@hotmail.com)

This work was supported in part by the National Natural Science Foundation of China under Grant 51907028, in part by the Jiangsu Provincial Key Laboratory of Smart Grid Technology and Equipment, in part by the Beijing Natural Science Foundation under Grant 3182041, and in part by the Jiangsu Planned Projects for Postdoctoral Research Funds.

ABSTRACT Stator turn fault is the most serious failure in the electrical machine drive which requires immediate detection techniques. Under such a turn fault, the fundamental change is that the high frequency (HF) impedance of the fault phase is significantly reduced due to the flux nullifying effect of the fault turns. Thus, this paper proposes a novel turn fault detection technique by using the equivalent HF impedance. It is derived by the HF voltage and current signals which are obtained by processing the phase voltages and currents with a bandpass filter. The effectiveness of the proposed is verified by extensive simulation and experimental tests on both surface mounted and interior PM machines. It is demonstrated that the performance of the proposed detection method is superior than the conventional HF current ripple based method. The investigation also confirms that the fault can be detected at an early stage by the proposed method.

INDEX TERMS Turn fault detection, high frequency, current harmonic, voltage harmonic, impedance, bandpass filter.

I. INTRODUCTION

In the electrical machine drives [1], stator turn fault was commonly referred as the worst fault scenario [2]. It was caused by accumulative winding insulation degradation and finally develops to a turn-to-turn short circuit fault. The impedance of the short-circuited loop is extreme low and it will results in large fault current in the fault turns [3]. The excessive fault current will cause rapid temperature rise and may lead to catastrophic failure. Therefore, fast and reliable turn fault detection is of key importance for the electrical machine drives to trigger the protection action [4].

It is worth noting that there are several possible fault scenarios in the machine drive, including the switch open circuit, short circuit fault and stator winding turn fault [5]. The diagnosis of the open circuit and short circuit fault is relatively easy. The open circuit fault can be detected by analyzing the phase current waveform and the switch on/off state while the short circuit can be alarmed by monitoring the overcurrent [6]. Thus, the stator turn fault becomes the most challenging fault for diagnosis [7].

The turn fault detection techniques have been the research hotspot for decades [8]. They can be generally classified as two approaches, one is based on the low frequency signals and the other is based on the high frequency signals. The low frequency signal based approach is using motor current signal analysis (MCSA) concept to spot the winding insulation breakdown [9]. In [10], the stator turn fault detection is realized by using the 2^{nd} harmonics in the instantaneous active/reactive power for the generating/ motoring modes, respectively. In [11], the third harmonic in line current was employed as fault indicator for a brushless DC machine drive. It should be noted that majority of existing techniques are based on the low frequency components [12], such as the fundamental component, the second or the third harmonics. Some novel smart methods in [13], [14] can be referenced to extract and process the fault signals for detection purpose.

Due to the merits of independent with the speed and load conditions, high frequency (HF) injection technique can be exploited for fault diagnosis which was first studied in [15]. A HF carrier signal was superimposed on the fundamental

The associate editor coordinating the review of this manuscript and approving it for publication was Dazhong Ma.

voltage. Then, the stator turn fault was detected by monitoring the dc component in the negative sequence carrier signal current which indicates the stator stationary saliency. In [16] it was found that the zero sequence carrier signal voltage also can be employed for turn fault detection. A desirable merit of the HF signal based detection technique is that the machine speed and load has little influence on the signals. For machine with salient rotor, it reacts with the HF voltage harmonic and results in secondary spatial harmonics which limits the application. The above method is improved by injecting the pulsating voltage on the d-axis in [17]. As a result, the induced currents are decoupled with the rotor saliency and the fault diagnostic performance is enhanced.

It should be noted that the above HF injection method introduces undesirable effects on the machine drive, such as increased losses, noises and voltage/current harmonics. It also reduces the available voltage which deteriorates the machine high speed performance. As a result, an advanced method was proposed in [18] by employing the inverter switching harmonics as a natural source of HF signal for the motor. No additional HF voltage harmonic injection is required and the undesirable effects are therefore eliminated. The induced HF PWM ripple currents are compared between different phases to indicate the turn fault. However, it is assumed that the applied voltages are still identical for different phases which is obviously not true in the postfault operation condition. The applied voltages vary with the fault location, number of fault turns, etc. Therefore, the voltage signals should also be considered to improve the fault detection capability. In [19], the turn fault is detected by monitoring the zero sequence HF PWM voltage. And the classification with the high resistance fault is analyzed by distinguishing the high frequency and low frequency components. In [20], the turn fault is monitored by analyzing the sidebands distribution of the common mode HF PWM voltages. As a result, the fault location and fault severity can be estimated.

According to the above literature review, it can be concluded that for the diagnosis techniques based on the low frequency signals, the frequencies of the targeted signals are close to the fundamental components, it increases the difficulty to segregate the fault signals. And the voltage/current signals are susceptible to be affected by the number of fault turns, external fault resistance, operation condition, resulting in an unpredictable detection manner [21]. In terms of the HF voltage harmonic injection based detection method, it is immune to the machine operation conditions, including the speed and load transients. However, it introduces additional noise, vibration and loss to the machine drive. For the PWM harmonic based fault detection, it does not introduce any additional voltage harmonics and hence avoids these unfavorable disadvantages. And, it is worth noting that for the current-state-of-art, the existing HF signal based turn fault detection techniques only exploit the current or voltage signals only which make the fault signals not strong enough [22]. In fact, both the HF current and voltage signals are affected by the fault which contain the fault information. And the fundamental change after the turn fault is that the impedance is significantly reduced [23], especially in the HF range where the influence of the resistance is eliminated.

Thus, this paper first time attempts to use the concept of equivalent high frequency impedance as fault indicator for stator turn fault detection. Both the HF current and voltage induced by the PWM operation are processed to derive the equivalent HF impedance. The equivalent HF impedances of different phases are compared to indicate the fault. It will be demonstrated that the proposed method exhibits higher signal noise ratio than the PWM ripple current based technique in [22] which only explore the HF current signals. In addition, it is insensitive to the external fault resistance, therefore, it can detect the fault at an early stage.

II. HF IMPEDANCE BASED TURN FAULT DETECTION DESIGN

Fault detection is usually based on the physical quantity change in the machine drives, like the voltage, current, power, etc. Impedance is a unique feature of the electric machine drives which describes the relationship of the applied voltage against the induced current. It contains reach information of the winding circuit connection which is suitable for fault indication [24]. This paper focuses on the HF impedance variation due to the turn fault. Thus, the phase impedance before and after a turn fault is analyzed first. For a healthy machine phase winding, it can be represented as a resistance and inductance circuit in series [18]. Its impedance is written as in (1).

$$Z_h = R + j\omega L \tag{1}$$

The resistance R and inductance L are 0.68Ω and 2.8mH, respectively for a surface mounted PM machine. Obviously, the phase impedance increases with the excitation frequency ω as the voltage drop on the inductance part increases. The impedance variation with the frequency is plotted in FIGURE 2 for the healthy condition.

In case of healthy condition, the current flowing in the $N - N_f$ and N_f turns is the same denoted as i_h. The phase flux linkage can be expressed as in (2).

$$\psi_1 = \left(L_h + 2M_{hf} + L_f\right) i_h \tag{2}$$

In case of a turn fault, the phase winding branch is illustrated as in FIGURE 1. An ideal short circuit fault occurs in the N_f turns out of total N turns in the phase winding. The fault turns ratio is defined as μ. The R_h, R_f, L_h, L_f are the resistance and inductance of the healthy and fault turns, respectively and M_{hf} is the mutual inductance between the two parts. The values of the parameters with 2 turns fault and 20 turns fault are listed in Table 1 according to finite element simulation. The details of the machine specifications can be found in [18].

After the turn fault, the currents in the two branches are no more the same. Here the same current i_h is assumed in the healthy $N - N_f$ turns. Due to the turn short circuit fault, the voltage, viz. the flux linkage of the fault N_f turns is

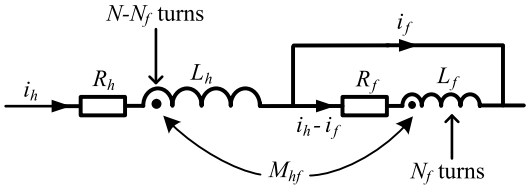

FIGURE 1. Schematic of the phase winding under turn fault.

TABLE 1. Phase winding parameters under fault conditions.

Parameter	Fault condition	
N_f	2 turns/62 turns	20 turns/62 turns
R_h	0.66Ω	0.46Ω
R_f	0.02Ω	0.22Ω
L_h	2.6mH	1.3mH
L_f	2.8μH	0.28mH
M_{hf}	83μH	0.6mH

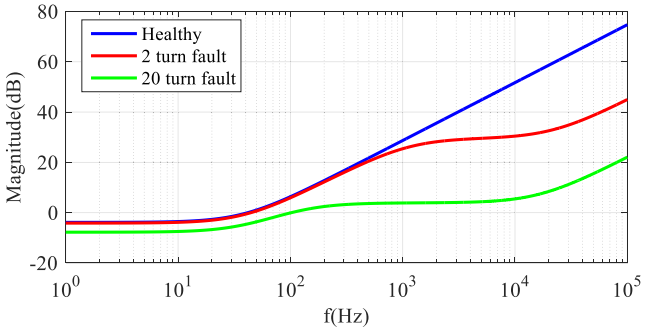

FIGURE 2. Magnitude of the phase impedance under healthy and turn fault conditions.

zero. Hence, the equation (3) can be obtained. As a result, the current $(i_h - i_f)$ in the fault N_f turns can be derived as in (4).

$$\psi_f = M_{hf} i_h + L_f (i_h - i_f) = 0 \tag{3}$$

$$i_h - i_f = -\frac{M_{hf} i_h}{L_f} \tag{4}$$

Hence, the phase flux linkage after the fault can be represented as in (5). Obviously, it is reduced by the short circuit fault current. In other words, it is nullified by the turn short circuit fault.

$$\begin{aligned}\psi_2 &= (L_h + M_{hf}) i_h + (L_f + M_{hf}) \left(-\frac{M_{hf} i_h}{L_f}\right) \\ &= L_h i_h - \frac{M_{hf}^2 i_h}{L_f}\end{aligned} \tag{5}$$

Consequently, the phase impedance after the turn fault can be derived as in (6).

$$Z_f = R_h + j\omega L_h + \frac{\omega^2 M_{hf}^2}{R_f + j\omega L_f} \tag{6}$$

The phase impedance under turn fault conditions is also plotted in FIGURE 2. It is seen that the phase impedance increases with the frequency. However, it is significantly lower when compared with the healthy condition in the high frequency range (>10kHz).

As explained above, it is because the short circuit loop reacts as a superconducting coil and the induced fault current always tries to counteract the external flux and maintain the total flux linkage as constant, commonly referred as flux nullifying effect. The flux nullifying effect only takes place when there is a short circuited path in the machine phase windings. The short circuit current in the fault part will produce a flux linkage with opposite direction of the external flux linkage. Consequently, the total phase flux linkage and the phase voltage is reduced, leading to reduced impedance.

And the impedance decreases with the number of the fault turns. With more short circuited turns, the flux nullifying effect of the fault turns is enhanced and further reducing the phase voltage, resulting in lower impedance. If all the phase winding turns are short circuited, the impedance will be reduced to zero.

With the fact of the reduced phase impedance under turn fault condition, the HF ripple current due to the inverter PWM operation is utilized for fault detection in [18], [22]. The filtered PWM ripple current of different phases are compared with each other to indicate the fault. It is assumed that the applied HF voltage on different phases are still identical which is not true under turn fault conditions. The phase voltages is distorted by the fault and will definitely affect the HF voltages [10]. It will be demonstrated that in turn fault condition, the HF current of the fault phase increases and the opposite is true for the HF voltage. Thus, both the HF current and voltage signals contain the fault information and therefore should be considered. As a result, this paper proposes the equivalent HF impedance for turn fault detection which combines both the HF voltage and current information. The equivalent HF impedance Z_e will result in a stronger fault indicator than using the HF current only. The equivalent HF impedance can be obtained by (7).

$$Z_e = \frac{U_{HF}}{I_{HF}} \tag{7}$$

The FIGURE 2 represents the accurate phase impedance under each frequency which requires the exact voltage and current signals under the specific frequency. However, in reality, the PWM operation of the inverter phase legs produces a wide range spectrum voltage harmonics from a few kHz to several tens of kHz. It is very difficult to extract a single HF frequency signal for both the HF voltage and current to obtain the impedance under a specific frequency for online processing. Hence, the HF signal spectrum produced by the PWM operation is analyzed.

Here the standard 3-phase inverter is utilized for machine drive [25] and SVPWM is employed for higher dc voltage utilization ratio. For the purpose of illustration, the switching frequency is set as 10 kHz while the modulation index is set as 0.6 for 100V dc bus voltage. The measured phase voltage is shown in FIGURE 3 which obviously contains rich PWM

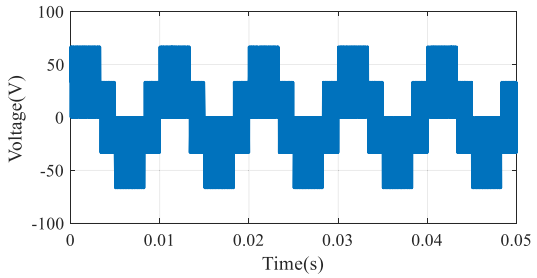

FIGURE 3. Phase PWM voltage.

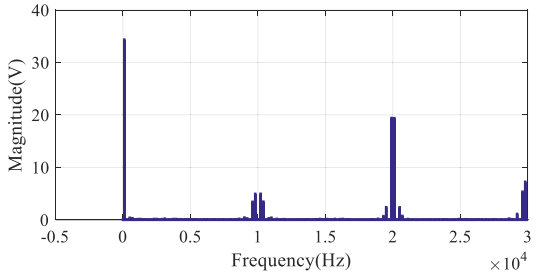

FIGURE 4. Spectrum of phase PWM voltage.

harmonics. Its spectrum is analyzed by fast Fourier transform and plotted in FIGURE 4. The frequency components higher than 30 kHz are not shown, since their amplitudes and induced ripple currents are much lower and can be neglected.

It is seen that majority of the PWM voltage harmonics are distributed symmetrically around the integer multiples of the switching frequency and form several sideband clusters. For the equivalent HF impedance based detection, it is desirable to separate the targeted frequency with maximum signal amplitude and minimize the influence of other harmonics. However, it is very difficult to separate a single frequency component within a sideband cluster. Therefore, the frequencies around one cluster, viz. from 19 kHz to 21k Hz, which can be separated by a bandpass filter, are processed as a whole. According to FIGURE 4, the sideband cluster around 20 kHz has the highest magnitude and therefore it is selected as the center frequency of the bandpass filter.

To extract the required HF voltage and current harmonics from the sensor-measured physical signals, which include the fundamental component and other high frequency harmonics, a second order bandpass filter is designed with the center frequency at 20 kHz with bandwidth of 2 kHz. The bode plot of the bandpass filter is shown in FIGURE 5. It is seen the filter provides sufficient attenuation for both the higher and lower order harmonics. So the influence of the fundamental components and the other high order components are minimized. Meanwhile, the gain of the pass band around 20 kHz is 30 dB which is good enough to extract the targeted frequency components. The filtered voltage and current signal is then sent to a RMS detector and a lowpass filter to measure its magnitude as shown in FIGURE 6. Subsequently, the equivalent HF impedance can be derived by (7) and the turn fault can be detected by comparing between different

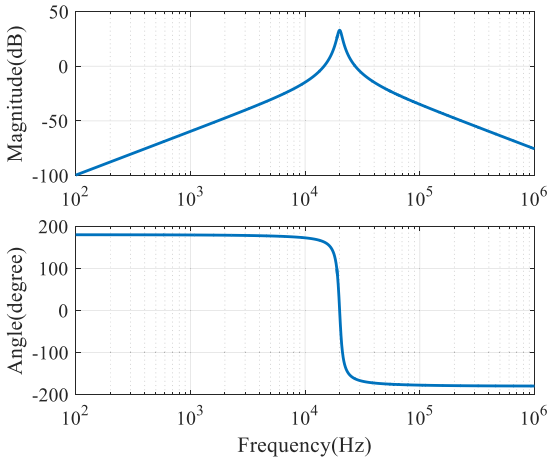

FIGURE 5. Bode plot of bandpass filter.

FIGURE 6. HF voltage and current measurement diagram.

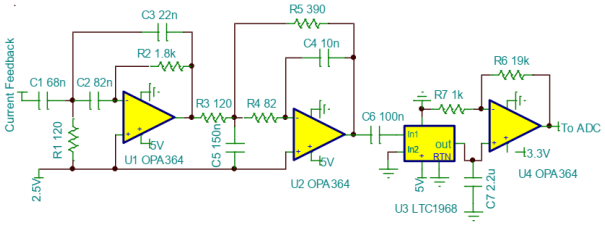

FIGURE 7. Bandpass filter circuit implementation.

phases. The filter function is realized by an analog circuit as shown in FIGURE 7 using analog chips. The detail of the PCB design can be found in [18], [22]. Thus, the time delay of the bandpass filter is negilible. Then, the extracted HF voltage and current signals are sampled by ADC ports of the DSP board where the HF impedances are calculated. In the DSP controller, the turn fault can be detected by comparing the HF impedances of different phases. And fault mitigation measure can be taken to protect the machine drive.

Strictly speaking, the value obtained by (7) is not impedance at a specific frequency, however, it represents the magnitude of the phase winding impedance in a small HF range. So it is called as equivalent HF impedance. The change in the equivalent HF impedance contains the fault signal which can be employed for fault detection. The effectiveness of the proposed method will be validated by extensive simulation and experimental tests.

III. SIMULATION STUDY

A. MACHINE MODELLING

In this section, the proposed turn fault detection by using equivalent HF impedance is verified by MATLAB simulation. The detection performance is compared with the

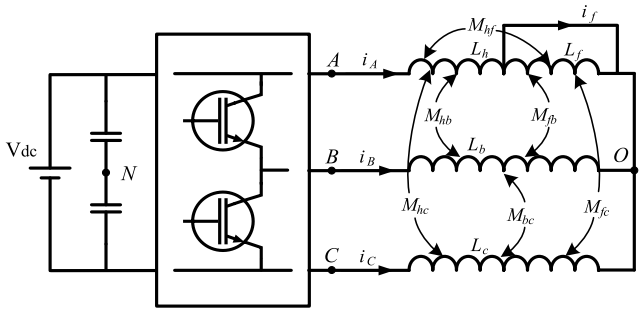

FIGURE 8. Schematic circuit of 3 phase machine with inverter.

TABLE 2. Simulation parameters of SPM and IPM.

	R	PM flux linkage ψ_m	L_d	L_q
IPM	0.06Ω	0.05Vs	0.55mH	1.45mH
SPM	0.06Ω	0.1Vs	0.55mH	0.55mH

conventional PWM ripple current based method, which only explores the HF current signal only [18], [22]. Without loss of generality, the effectiveness of the proposed detection method is investigated for both the surface mounted PM machine (SPM) and the interior PM machine (IPM). Their electrical parameters are provided in Table 2. The schematic circuit of the 3-phase machine drive is illustrated in FIGURE 8. The phase self-inductances and mutual-inductances can be derived by L_d and L_q according to [19]. A turn fault is assumed in phase A and the fault turns ratio μ is 0.1 for both machines. The fault turns are ideally short circuited since the external resistance becomes negligible when compared with the HF impedance of the fault turns. The faulty machine together with the 3-phase full bridge circuit is implemented in MATLAB/ SIMULINK environment. The machine drive is under closed loop current control to track the current commands. And SVPWM is employed for the inverter switches modulation, the switching frequency is set as 10 kHz.

B. TURN FAULT SIMULATION WITHOUT EXTERNAL RESISTANCE

First, the simulation is performed on the SPM drive. Initially, the machine is operating in healthy condition at 100Hz electrical frequency. The loaded currents are $i_d = 0$A, $i_q = 60$A. At 0.1s, an ideal short circuited turn fault is injected in phase A. the induced turn fault current and the three phase currents are plotted in FIGURE 9. It is seen that the fault current shoots to 1000A after the turn fault. The phase currents become slightly distorted though they are under the closed loop current controller. In addition, the HF current ripples increase after the turn fault. Obviously, the magnitude of the HF current ripple in phase A is the highest.

Meanwhile, the phase PWM voltages are shown in FIGURE 10. It is very difficult to observe useful information from it, so the phase voltage references are also plotted which is more representative. The phase voltage references are symmetrical before the turn fault and notable distortion is

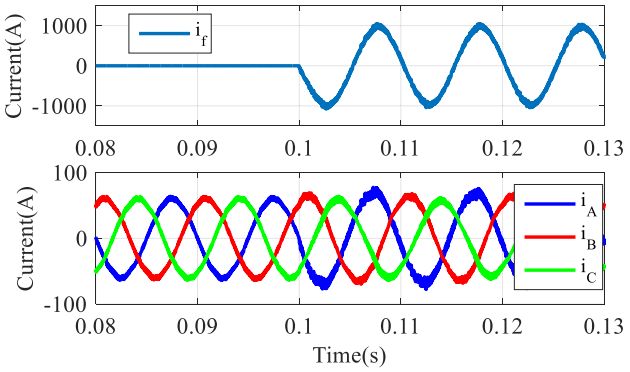

FIGURE 9. Fault current and phase currents of SPM.

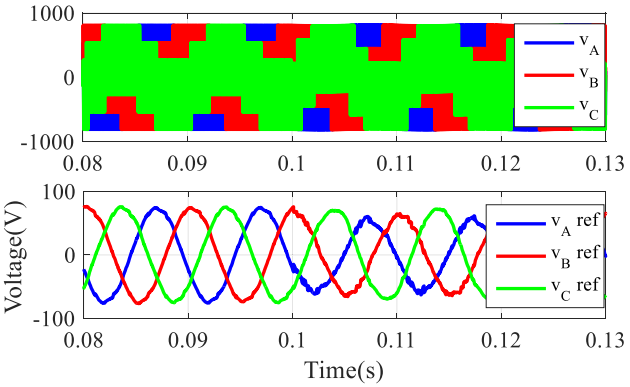

FIGURE 10. Phase voltages and voltage references of SPM.

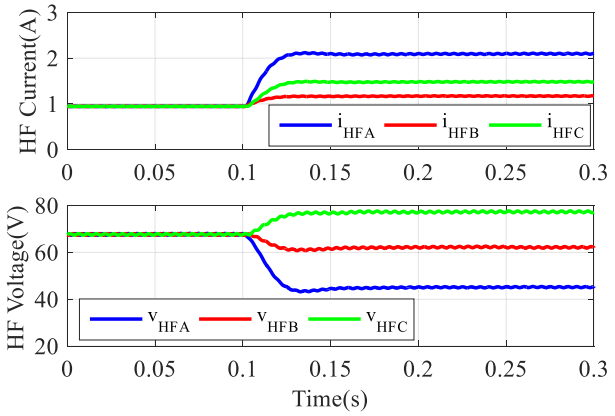

FIGURE 11. Filtered phase currents and voltages of SPM.

observed after the fault. The magnitude of the voltage on the fault phase A is lower than the other healthy phases. It indicates that the applied HF voltage on the phases are no more identical. Therefore, simply comparing the HF current ripple will not lead to optimal detection performance since it does not capture the fault features in the phase voltage excitations. Thus, the HF voltage signals should also be included.

Hence, both the phase currents and voltages are processed by the bandpass filters as in Section II. The filtered HF current and voltage signal are plotted in FIGURE 11. It is seen that

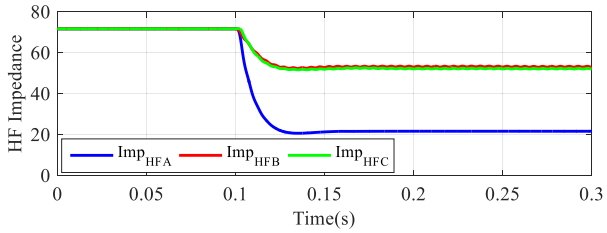

FIGURE 12. Equivalent HF impedance of SPM.

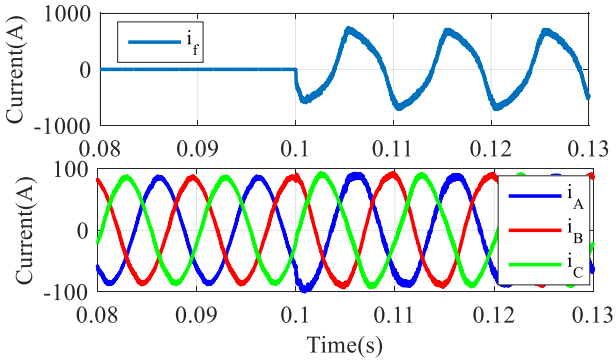

FIGURE 13. Fault current and phase currents of IPM.

the magnitudes of the three phase HF current signals are different after the fault. It is mainly because when a fault occurs, the applied phase voltages are no longer symmetrical which affect the HF voltage harmonics. It is found the HF current of the fault phase A is the highest. The ratio between the maximum and minimum values of the three phases is 1.8.

In terms of the HF voltage signals, they also deviate from each other after the fault due to the voltage distortion. It is observed that the HF voltage of the fault phase A is the lowest. Considering the fact that the HF current of phase A is the highest, it leads to the equivalent HF impedance of phase A is the lowest. The three phases equivalent HF impedances are derived by equation (7) and plotted in FIGURE 12. Obviously, the equivalent HF impedance of phase A is the lowest, and the ratio between the maximum and minimum values of the three phases is 2.46. The fault signal ratio is increased by 37% than using HF current signal only. Thus, the fault detection performance is significantly enhanced.

The same study has been performed on an IPM drive. The machine is also operating at 100Hz electrical frequency. In order to explore the reluctance torque, The loaded currents are set as $i_d = -60$A, $i_q = 60$A. The turn fault is also injected in phase A at 0.1s. The simulated results, including the fault current, phase currents, phase voltages and references, filtered signals and derived equivalent HF impedances are provided as shown in FIGURE 13-FIGURE 16. Similar trends are found on the IPM drive. After the turn fault, the HF current ripple of the fault phase A increases. The ratio between the maximum and minimum values of the three phases is 2 as shown in FIGURE 15. This ratio may be caused by the different applied voltage as shown in FIGURE 14. The final

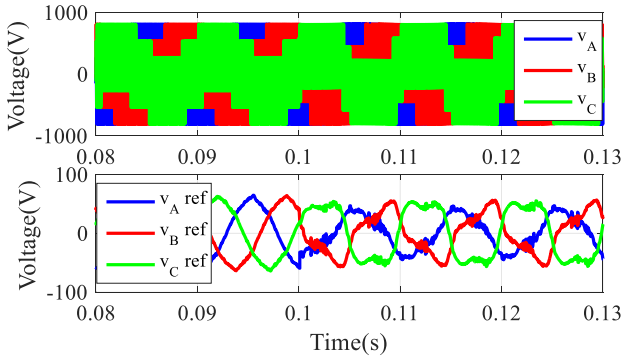

FIGURE 14. Phase voltages and voltage references of IPM.

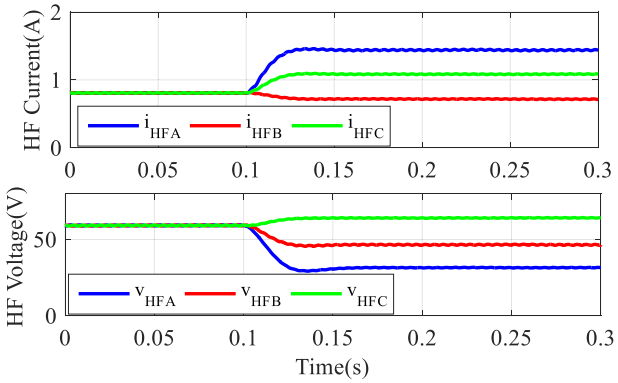

FIGURE 15. Filtered phase currents and voltages of IPM.

derived three phases equivalent HF impedances are given in FIGURE 16. The ratio between the maximum and minimum values of the three phases is 2.96 which is also increased by ∼50%. As a result, the fault detection performance is also improved.

C. TURN FAULT SIMULATION WITH EXTERNAL RESISTANCE

The turn fault is developed by gradual degradation of the insulation resistance from mega-ohms to a few milliohms. As known to all, the turn fault current increases with the decrease of the insulation resistance. Therefore, it would be desirable it can be detected at an early stage with small fault current which does not cause catastrophic failure to the machine drive. However, the early diagnosis is very challenging since the fault current and the induced fault signal are small [10]. Nonetheless, the HF signal based detection method is insensitive to the external fault resistance. In another words, The turn fault could be detected at an early stage to avoid excessive large fault current. Thus, the turn fault has been simulated for the SPM drive with additional 100mΩ resistance in the short circuited loop as shown in FIGURE 17.

The simulated results are provided as shown in FIGURE 18∼FIGURE 19. With the additional 100mΩ resistance, the magnitude of the fault current is notable reduced.

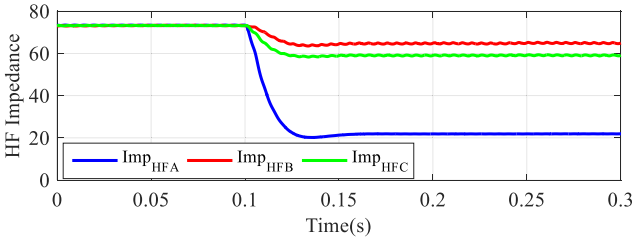

FIGURE 16. Equivalent HF impedances of IPM.

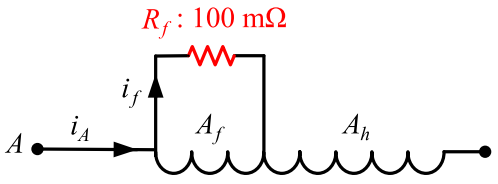

FIGURE 17. Turn fault with additional 100 mΩ external resistance.

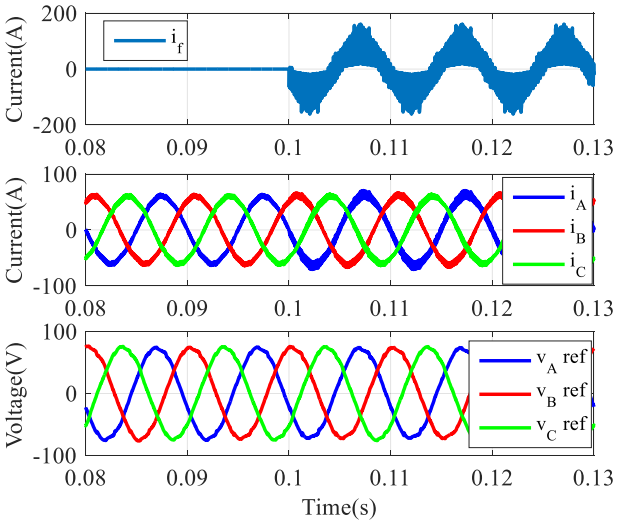

FIGURE 18. Fault current, phase currents and phase voltage references of SPM with 100mΩ resistance.

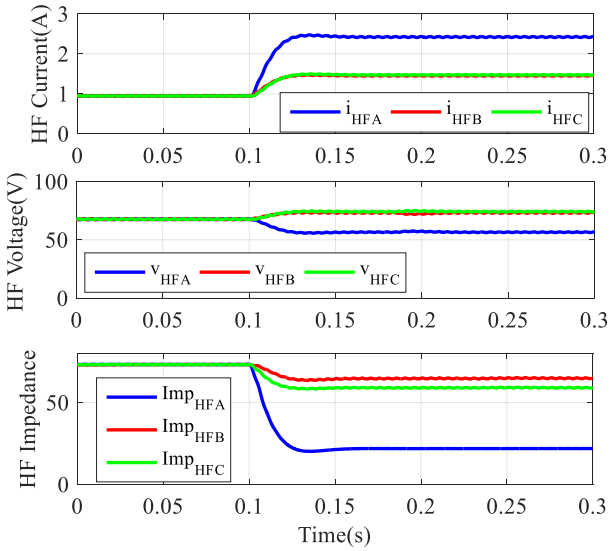

FIGURE 19. Filtered phase currents, voltages and equivalent HF impedances of SPM with 100mΩ resistance.

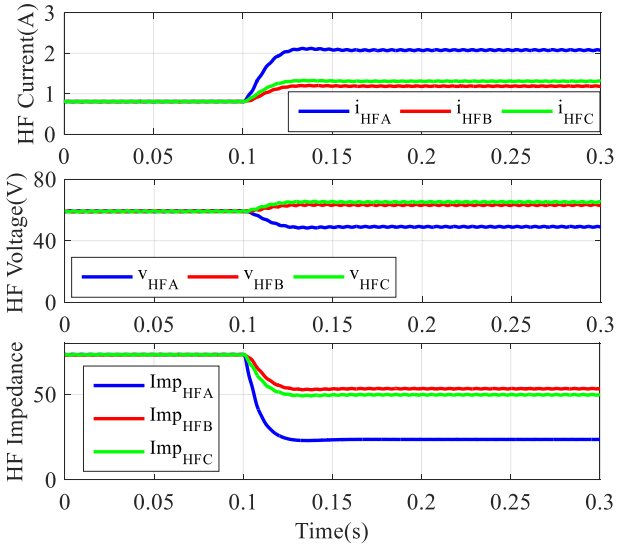

FIGURE 20. Filtered phase currents, voltages and equivalent HF impedances of IPM with 100mΩ resistance.

The phase currents are still well controlled and the voltage reference values are less distorted. In terms of the HF signals, the HF current ripple in the fault phase A is still the highest. The ratio between the maximum and minimum values of the three phases is 1.67, slightly lower than the ratio in FIGURE 11. In the filtered HF voltage signals, the differences between the three phases are smaller than those in FIGURE 11. It is because the fault current is lower and the phase voltages are less distorted. For the final derived equivalent HF impedances, the ratio between the maximum and minimum values of the three phases is 2.16 which is 30% higher than using the HF current signal only. It confirms that the proposed technique can detect the fault earlier than the conventional PWM ripple current based method.

The same analysis has been repeated on the IPM drive with 100mΩ external resistance. The filtered phase currents, voltages and equivalent HF impedances are provided as shown in FIGURE 20. Similar trends are observed. The ratio between the maximum and minimum value of the HF currents and the equivalent HF impedances are 1.75 and 2.26, respectively. The ratio of the equivalent HF impedance based method is 30% higher than the HF current based method, demonstrating better detection capability. As a result, the fault can be detected at an early stage avoiding catastrophic failure. This merit is desirable which cannot be achieved on the low frequency signal based detection method.

IV. EXPERIMENTAL TEST

The equivalent HF impedance based turn fault detection is verified on a triple redundant 3-phase IPM drive as shown in FIGURE 22 [26], the machine specification is provided

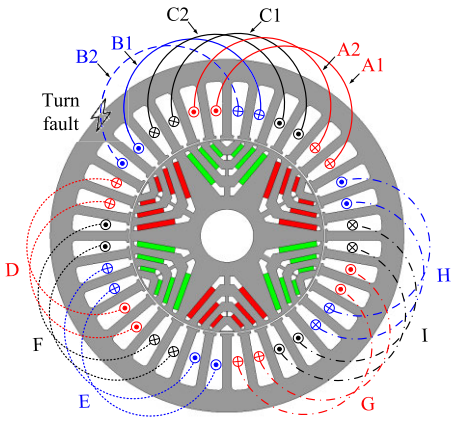

FIGURE 21. Triple redundant 3-phase IPM with non-overlapped windings.

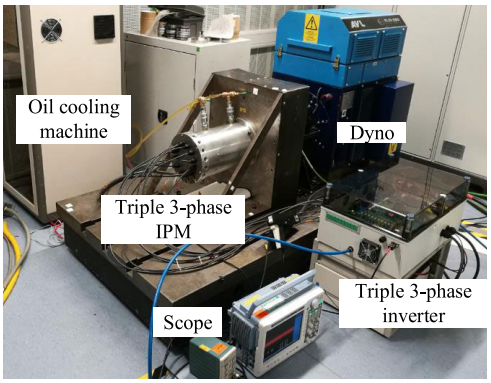

FIGURE 22. Test bench of the prototype machine drive.

in Table 3. The IPM drive is equipped with three isolated 3-phase windings to improve the fault tolerant capability. Each 3-phase winding set is driven by an independent full bridge inverter. This machine is capable of uninterrupted operation in case of a turn fault on one 3-phase set. Therefore, fast and reliable turn fault detection technique is essential for this type of machine to activate the mitigation action and enable the fault tolerant operation [27].

As shown in FIGURE 22, the machine is connected to the dynamometer via an inline torque transducer rotating at a given speed. The machine is fed by a DSP based 9-phase inverter. The inverter switches operate at 10kHz in SVPWM mode. In order to test the turn fault behavior in a controlled manner, taps for a single turn fault are brought out from coil B2 of set ABC as shown in FIGURE 23(a). The taps are connected via thick cables to a high current relay to emulate the turn fault as shown in FIGURE 23(b). The machine phase current and voltage signals are measured at by a high precision YOKOGAWA oscilloscope DL850. The measured current and voltage signals are processed by the bandpass filter as designed in section II [18], [22]. It should be noted that here only the signals of the fault set ABC are processed and presented, the healthy sets DEF and GHI are not shown since they are almost not affected by the turn fault.

TABLE 3. Specifications of the triple redundant 3-phase machine.

Specification	Symbol	Value
Base speed	n_b	4 000 rpm
Maximum speed	n_m	19 200 rpm
Rated power	P_r	35 kW
Rated current and gamma angle	I_{rated}	120 A (51°)
Nominal DC link voltage	V_{dc}	270 V
Turn number of each coil	N	8
Faulty turn number	N_f	1

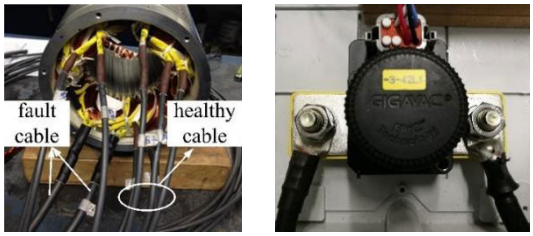

FIGURE 23. Stator turn fault test setup (a) cable leads (b) fault control relay.

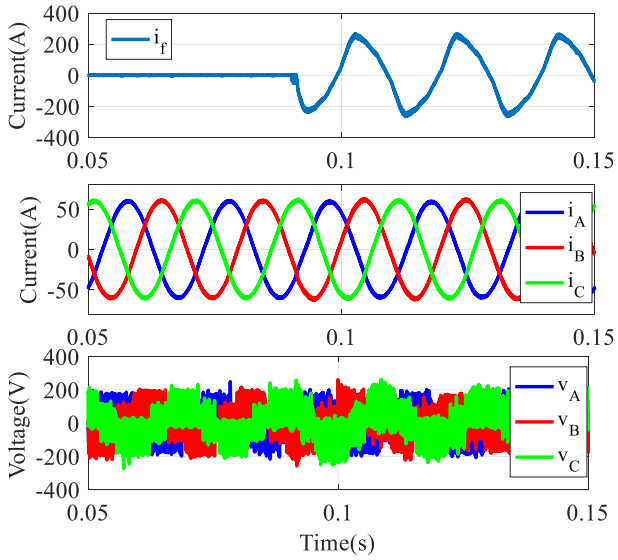

FIGURE 24. Measured turn fault current, phase currents and voltages at 1000rpm with 60A currents.

A. TURN FAULT TEST WITHOUT EXTERNAL RESISTANCE

For the purpose of safe operation, the equivalent HF impedance based detection is first verified at 1000rpm, otherwise the excessive turn fault current may damage the whole machine. Initially, all three 3-phase sets are excited 60A currents in Maximum Torque per Ampere (MTPA) condition. Then a turn fault is injected at 0.09s as shown in FIGURE 24 by closing the fault control relay in FIGURE 23(b), it shoots to 260A. The phase currents and voltages of set ABC are also shown which are well controlled by the closed loop controller with small distortion after the turn fault. It implies that the turn fault is very difficult to be detected if using the low frequency signals. The voltage and current signals are processed by the bandpass filter in FIGURE 7. The filtered

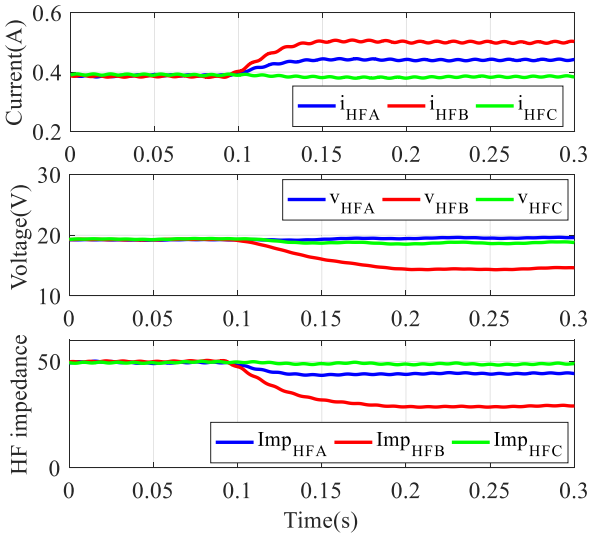

FIGURE 25. Measured HF currents, HF voltages and equivalent HF impedances at 1000rpm with 60A currents.

HF currents, HF voltages and equivalent HF impedances are provided in FIGURE 25. The waveforms are very close with the simulation results with small amplitude differences. In healthy condition, the amplitudes of the HF voltages and currents are very close, leading to similar HF impedances for different phases. After the turn fault, it is seen that the HF current of the fault phase B is the highest and vice versa for the equivalent HF impedance. The ratio between the maximum and minimum values of the three phase HF currents and the equivalent HF impedances are 1.3 and 1.68, respectively. Thus, the equivalent HF impedance based detection method is capable to detect the fault, and has increased the fault signal ratio by 30%, indicating better detecting capability.

B. VERIFICATION WITH DIFFERENT SPEED AND CURRENT

The proposed method has been examined in a wide operation range by varying the speed and load currents. Thus, the previous test has been extended from 500rpm to 1500rpm by varying the load current from 20A to the rated 120A. The HF voltage and current signals are processed in the same way. The obtained fault signal ratios of the HF current based method and the equivalent HF impedance based method are compared in FIGURE 26. It is found that in ratio of the equivalent HF impedance based method is always about 30% higher than that of the HF current based method. It confirms that the proposed method improves the turn fault detection capability in a wide operation range. And the higher the speed, the larger the fault signal ratio. Thus, the fault will be reliably detected at high speed.

The threshold value of the fault signal ratio has a fundamental impact on the detection performance, like the response time, accuracy, etc. It could be determined by analyzing the fault signal ratios in healthy and fault conditions. According to the analysis in FIGURE 24 and FIGURE 25, it is seen the fault signal ratio, which is the maximum HF impedance value over the minimum value, in healthy condition is very

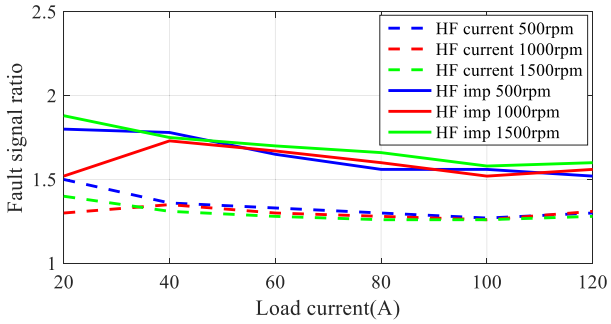

FIGURE 26. Fault signal ratio comparison of the HF current based method and the equivalent HF impedance.

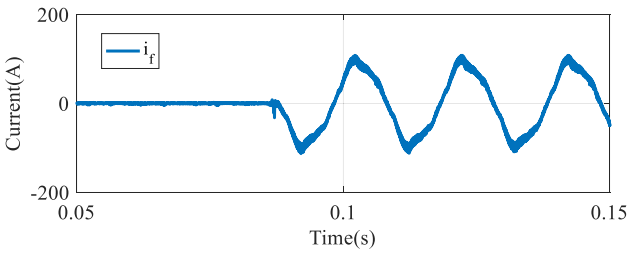

FIGURE 27. Measured turn fault current at 1000rpm with 60A currents with 10 mΩ fault resistance.

close to 1. In fault conditions, according to the investigation in FIGURE 26, it is seen the fault signal ratio is always higher than 1.5 under 500rpm, 1000rpm, 1500rpm operation. Therefore, the threshold value can be determined as 1.2. The detection time in FIGURE 25 is no more than 25ms. This threshold value is good enough to have fast response time and high accuracy.

It is worth noting that the HF signals are affected by the DC bus voltage, switching frequency, modulation index. This trend has been studied in [22]. However, the proposed method utilizes the ratio between the maximum value and minimum value. The HF voltages, currents and the resultant impedance signals of different phases are affected in the same way by the above factors. Hence, the influences is minimized. In addition, a commission operation is recommended to consider the inherent asymmetry in the phase winding and filter circuit.

C. TURN FAULT TEST WITH EXTERNAL RESISTANCE

Turn fault with zero external resistance is an ideal case. In fact, there is always a contact resistance with about several milliohms. Thus, the turn fault has also been tested with additional 10 mΩ resistance in the short circuited loop when the machine operates at 1000rpm with 60A load current. The resultant turn fault current is shown in FIGURE 27. As expected, the fault current reduces to 100A compared with FIGURE 24. With the same bandpass filter processing, the filtered HF currents, HF voltages and equivalent HF impedances are shown in FIGURE 28. Due to the external resistance, the measured signals all decrease. The ratio between the maximum and minimum values of the three phase HF currents and the equivalent HF impedances

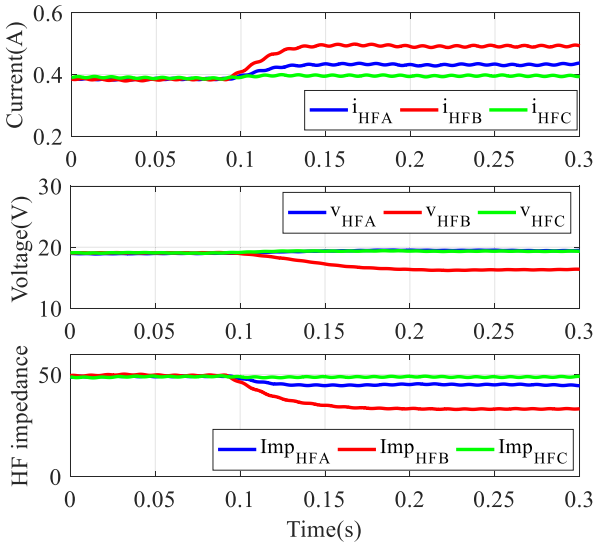

FIGURE 28. Measured HF currents, HF voltages and equivalent HF impedances at 1000rpm with 60A currents with 10 mΩ fault resistance.

are 1.24 and 1.47, respectively. Thus, the equivalent HF impedance based detection method can still detect the fault with stronger fault signal. Hence, the fault can still be detected in phase B at an early stage and therefore avoiding catastrophic failure.

V. CONCLUSION

In this paper, an equivalent HF impedance based turn fault detection method is proposed and investigated. The underlying fundamental theory is the impedance of the fault phase is significantly reduced due to the flux nullifying effect of the short circuit fault turns. An analog bandpass filter is designed to filter the targeted frequency components. The effectiveness of the detection method has been validated by extensive simulations and experimental tests. The fault detection performance is compared with the conventional HF current ripple based method. It shows that the proposed method increase the fault signal ratio by about 30% in all operation range for both the SPM and IPM drive. And it is insensitive to the external fault resistance and therefore, can alarm the fault in an early stage which is desirable for the machine early diagnosis.

REFERENCES

[1] A. M. EL-Refaie, M. R. Shah, and K.-K. Huh, "High-power-density fault-tolerant PM generator for safety-critical applications," *IEEE Trans. Ind. Appl.*, vol. 50, no. 3, pp. 1717–1728, May 2014.

[2] A. H. Bonnett and G. C. Soukup, "Cause and analysis of stator and rotor failures in three-phase squirrel-cage induction motors," *IEEE Trans. Ind. Appl.*, vol. 28, no. 4, pp. 921–937, Jul. 1992.

[3] P. Arumugam, "Design optimization on conductor placement in the slot of permanent magnet machines to restrict turn–turn short-circuit fault current," *IEEE Trans. Magn.*, vol. 52, no. 5, pp. 1–8, May 2016.

[4] A. Gandhi, T. Corrigan, and L. Parsa, "Recent advances in modeling and online detection of stator interturn faults in electrical motors," *IEEE Trans. Ind. Electron.*, vol. 58, no. 5, pp. 1564–1575, May 2011.

[5] Q. Chen, W. Zhao, G. Liu, and Z. Lin, "Extension of virtual-signal-Injection-Based MTPA control for five-phase IPMSM into fault-tolerant operation," *IEEE Trans. Ind. Electron.*, vol. 66, no. 2, pp. 944–955, Feb. 2019.

[6] Q.-T. An, L.-Z. Sun, K. Zhao, and L. Sun, "Switching function model-based fast-diagnostic method of open-switch faults in inverters without sensors," *IEEE Trans. Power Electron.*, vol. 26, no. 1, pp. 119–126, Jan. 2011.

[7] S. Afrandideh, M. E. Milasi, F. Haghjoo, and S. M. A. Cruz, "Turn to turn fault detection, discrimination, and faulty region identification in the stator and rotor windings of synchronous machines based on the rotational magnetic field distortion," *IEEE Trans. Energy Convers.*, vol. 35, no. 1, pp. 292–301, Mar. 2020.

[8] B. Du, S. Wu, S. Han, and S. Cui, "Interturn fault diagnosis strategy for interior permanent-magnet synchronous motor of electric vehicles based on digital signal processor," *IEEE Trans. Ind. Electron.*, vol. 63, no. 3, pp. 1694–1706, Mar. 2016.

[9] S. Nandi, H. A. Toliyat, and X. Li, "Condition monitoring and fault diagnosis of electrical motors—A review," *IEEE Trans. Energy Convers.*, vol. 20, no. 4, pp. 719–729, Dec. 2005.

[10] B. Wang, J. Wang, A. Griffo, and B. Sen, "Stator turn fault detection by second harmonic in instantaneous power for a triple-redundant fault-tolerant PM drive," *IEEE Trans. Ind. Electron.*, vol. 65, no. 9, pp. 7279–7289, Sep. 2018.

[11] S.-T. Lee and J. Hur, "Detection technique for stator inter-turn faults in BLDC motors based on third harmonic components of line currents," in *Proc. IEEE Energy Convers. Congr. Expo. (ECCE)*, Sep. 2015, pp. 1899–1904.

[12] B. Sen and J. Wang, "A fast detection technique for stator inter-turn fault in MultiPhase permanent magnet machines using model based approach," in *Proc. 7th IET Int. Conf. Power Electron., Mach. Drives (PEMD)*, 2014, pp. 1–6.

[13] R. Wang, Q. Sun, P. Zhang, Y. Gui, D. Qin, and P. Wang, "Reduced-order transfer function model of the droop-controlled inverter via jordan continued-fraction expansion," *IEEE Trans. Energy Convers.*, early access, 2020, doi: 10.1109/TEC.2020.2980033.

[14] W. Rui, S. Qiuye, M. Dazhong, and H. Xuguang, "Line impedance cooperative stability region identification method for grid-tied inverters under weak grids," *IEEE Trans. Smart Grid*, vol. 11, no. 4, pp. 2856–2866, Jul. 2020.

[15] F. Briz, M. W. Degner, A. Zamarron, and J. M. Guerrero, "Online stator winding fault diagnosis in inverter-fed AC machines using high-frequency signal injection," *IEEE Trans. Ind. Appl.*, vol. 39, no. 4, pp. 1109–1117, Jul. 2003.

[16] F. Briz, M. W. Degner, P. Garcia, and A. B. Diez, "High-frequency carrier-signal voltage selection for stator winding fault diagnosis in inverter-fed AC machines," *IEEE Trans. Ind. Electron.*, vol. 55, no. 12, pp. 4181–4190, Dec. 2008.

[17] S. C. Yang, "On-line turn fault detection of interior permanent magnet machines using the pulsating-type voltage injection," *IEEE Trans. Ind. Appl.*, vol. 52, no. 3, pp. 2340–2349, May/Jun. 2016.

[18] B. Sen and J. Wang, "Stator interturn fault detection in permanent-magnet machines using PWM ripple current measurement," *IEEE Trans. Ind. Electron.*, vol. 63, no. 5, pp. 3148–3157, May 2016.

[19] R. Hu, J. Wang, A. R. Mills, E. Chong, and Z. Sun, "Detection and classification of turn fault and high resistance connection fault in permanent magnet machines based on zero sequence voltage," *IEEE Trans. Power Electron.*, vol. 35, no. 2, pp. 1922–1933, Feb. 2020.

[20] H. Liu, J. Huang, Z. Hou, J. Yang, and M. Ye, "Stator inter-turn fault detection in closed-loop controlled drive based on switching sideband harmonics in CMV," *IET Electr. Power Appl.*, vol. 11, no. 2, pp. 178–186, Feb. 2017.

[21] Z. Ullah and J. Hur, "Analysis of inter-turn-short fault in an FSCW IPM type brushless motor considering effect of control drive," *IEEE Trans. Ind. Appl.*, vol. 56, no. 2, pp. 1356–1367, Mar. 2020.

[22] R. Hu, J. Wang, B. Sen, A. R. Mills, E. Chong, and Z. Sun, "PWM ripple currents based turn fault detection for multiphase permanent magnet machines," *IEEE Trans. Ind. Appl.*, vol. 53, no. 3, pp. 2740–2751, May 2017.

[23] J.-K. Park, C.-L. Jeong, S.-T. Lee, and J. Hur, "Early detection technique for stator winding inter-turn fault in BLDC motor using input impedance," *IEEE Trans. Ind. Appl.*, vol. 51, no. 1, pp. 240–247, Jan. 2015.

[24] S. Bin Lee, R. M. Tallam, and T. G. Habetler, "A robust, on-line turn-fault detection technique for induction machines based on monitoring the sequence component impedance matrix," *IEEE Trans. Power Electron.*, vol. 18, no. 3, pp. 865–872, May 2003.

[25] N. Bianchi, S. Bolognani, and M. Zigliotto, "Analysis of PM synchronous motor drive failures during flux weakening operation," in *Proc. PESC Record. 27th Annu. IEEE Power Electron. Spec. Conf.*, Jun. 1996, pp. 1542–1548.
[26] B. Wang, J. Wang, B. Sen, A. Griffo, Z. Sun, and E. Chong, "A fault-tolerant machine drive based on permanent magnet-assisted synchronous reluctance machine," *IEEE Trans. Ind. Appl.*, vol. 54, no. 2, pp. 1349–1359, Apr. 2018.
[27] B. Wang, J. Wang, A. Griffo, and B. Sen, "Experimental assessments of a triple redundant nine-phase fault-tolerant PMA SynRM drive," *IEEE Trans. Ind. Electron.*, vol. 66, no. 1, pp. 772–783, Jan. 2019.

BO WANG (Member, IEEE) received the B.Eng. and M.Sc. degrees in electrical engineering from the Nanjing University of Aeronautics and Astronautics, Nanjing, China, in 2009 and 2012, respectively, and the Ph.D. degree in electronic and electrical engineering from The University of Sheffield, Sheffield, U.K., in 2018.

From 2012 to 2014, he was a Senior Engineer with Delta Electronics Company Ltd. From 2017 to 2018, he was a Research Associate with the Department of Electronic and Electrical Engineering, The University of Sheffield. Since 2018, he has been with the School of Electrical Engineering, Southeast University. His research interests include permanent magnet machine drives, electric traction, and fault tolerant systems.

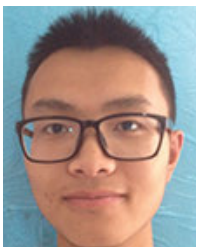

JIAPENG HU is currently pursuing the master's degree with Southeast University, Nanjing, China. He has received several prizes from the National Mathematical Modeling Competition.

GUANGHUI WANG (Member, IEEE) received the B.S. degree in electronic information engineering from the China University of Geosciences, Beijing, China, in 2005, and the Ph.D. degree in pattern recognition and intelligent system from the Beijing Institute of Technology, Beijing, in 2013.

Since 2013, he has been a Researcher with the China North Vehicle Research Institute. His research interests include development of electrical machine, servo control, artificial intelligence, and system engineering.

WEI HUA (Senior Member, IEEE) was born in Taizhou, China, in 1978. He received the B.Sc. and Ph.D. degrees in electrical engineering from Southeast University, Nanjing, China, in 2001 and 2007, respectively.

From September 2004 to August 2005, he visited the Department of Electronics and Electrical Engineering, The University of Sheffield, U.K., as a Joint-Supervised Ph.D. Student. Since 2007, he has been with Southeast University, where he is currently a Professor with the School of Electrical Engineering. He is the author or coauthor of over 150 technical articles. He holds over 50 patents in his areas of interest. His teaching and research interests include the design, analysis, and control of electrical machines.